Dynamics of *p*-Nitroaniline Molecules in Micoporous Aluminophosphate $AlPO_4$-5 Studied by Solid-State NMR

Yoshihiko Komori and Shigenobu Hayashi*

Research Institute of Instrumentation Frontier, National Institute of Advanced Industrial Science and Technology (AIST), Tsukuba Central 5, 1-1-1 Higashi, Tsukuba, Ibaraki 305-8565, Japan

Received: September 11, 2005; In Final Form: November 7, 2005

Dynamics of deuterated *p*-nitroaniline (pNA-*d*) molecules in the micropores of $AlPO_4$-5 has been investigated by means of solid-state NMR. The adsorbed amounts of pNA-*d* were 5.0 and 10.1 mass % of the total mass. We have measured ^{13}C magic-angle-spinning (MAS) and ^2H NMR spectra of the guest molecules and ^{31}P and ^{27}Al MAS NMR spectra of the host framework. The pNA-*d* molecules distribute rather inhomogeneously in the channel, and do not coordinate to Al strongly like H_2O. The intermolecular hydrogen bonds are formed between a part of the guest molecules only when the loading level is high. The ^2H NMR spectra are successfully analyzed, elucidating the orientation and the motion of the guest molecules. The molecular axis of pNA-*d* is inclined to the channel axis, and the molecular plane is perpendicular to the inner wall. The guest molecule jumps among 12 sites or 12 orientations. This motion is faster in the sample of 5.0 mass % than in the sample of 10.1 mass %, suggesting that the guest−guest interaction hinders the motion. The mean residence times of the molecules are estimated from the analysis of the ^2H NMR spectra, which are affected by the size of the nanospace as well as the property of the adsorbed site.

Introduction

Microporous materials have potential uses as new and intelligent materials, since the porous framework can accommodate various guest molecules. Zeolites and their analogues have extensively been used as the inorganic host materials, since they provide highly ordered pore structures with crystalline inorganic walls. The orientations of the guest molecules are constrained by the host. Extensive studies have been carried out on highly oriented arrangements of chromophores such as *p*-nitroaniline (pNA) in zeolites and microporous aluminophosphates.[1−8] The composite materials showed large nonlinear optical effects such as second harmonic generation (SHG) although neither component shows such effects. Characterization of the nanocomposites is one of the most important subjects for designing unique functional inorganic/organic materials with advanced performance.

$AlPO_4$-5 has one-dimensional channels of 12-membered rings with a diameter of 0.73 nm.[9] $AlPO_4$-5 containing pNA is a typical example of the nanocomposites. The $AlPO_4$-5/pNA system showed large SHG, which maximum was obtained at a loading amount of 13 mass %.[1] The orientation and dynamics of the guest molecules largely affect the SHG property. However, they are not well understood.

Solid-state NMR spectroscopy is advantageous for investigating dynamics and chemical environments of guest molecules. ^{13}C NMR can observe the organic guest molecules selectively and can probe the dynamics and chemical environments of the guest molecules.[10−13] ^2H NMR offers powerful approaches to investigate dynamics of molecules whose rate is of the order of 100 kHz.[14−16] Previously, we have investigated the dynamics of benzene, cyclohexane, and *n*-hexane in KL zeolite,[17] pNA in ZSM-5 zeolite,[18−20] acetonitrile and *n*-hexane in $AlPO_4$-5,[21] and pNA in mesoporous silica FSM-16.[22]

In the present work, we have studied the motion of pNA molecules in the micropores of $AlPO_4$-5 by means of solid-state NMR. In the framework of $AlPO_4$-5, AlO_4 and PO_4 tetrahedra connect with each other and there are no extraframework cations. The channel diameter is larger than that of ZSM-5 (about 0.54 nm) and much smaller than that of mesoporous FSM-16. We have measured ^{13}C magic-angle-spinning (MAS) and ^2H NMR spectra of the guest molecules and ^{31}P and ^{27}Al MAS NMR spectra of the host framework. We have successfully analyzed the ^2H NMR spectra, elucidating the orientation and the motion of the guest molecules

Experimental Section

Preparation of Materials. $AlPO_4$-5 was kindly supplied by Dr. K. Suzuki of AIST. Deuterated pNA (ring-d_4, pNA-*d*) was obtained from Cambridge Isotope Laboratories (Andover, USA).

Two kinds of $AlPO_4$-5/pNA-*d* samples with low and high loading amounts of pNA-*d* were prepared. $AlPO_4$-5 was dehydrated by evacuation at 473 K for 3 h before use. A weighed amount of pNA-*d* was introduced into $AlPO_4$-5 under nitrogen atmosphere. The sample tube sealed in vacuo was heated at 423 K for 6 h, after which the temperature was decreased to room temperature for 24 h.

In thermogravimeteric analysis (TGA), mass losses were 5.0 and 10.1 mass % for the low and high loading samples, respectively, which corresponded to the contents of pNA-*d* in $AlPO_4$-5.

Analyses. TGA was performed in air atmosphere by Rigaku Thermoflex TG8110 controlled by Rigaku Thermal Analysis Station TAS100. The heating rate was 10 K min^{-1}.

^{13}C MAS NMR measurements were carried out by a Bruker ASX400 spectrometer with a static magnetic field strength of 9.4 T. The Larmor frequency of ^{13}C was 100.61 MHz. A Bruker MAS probehead was used with a 7-mm zirconia rotor. The

* Address correspondence to this author. E-mail: hayashi.s@aist.go.jp.

10.1021/jp055130e CCC: $33.50
Published on Web 12/14/2005

spinning rate of the sample was set at 3.5 kHz to avoid the overlap of the isotropic peaks with the spinning sidebands. Chemical shifts were expressed with respect to neat tetramethylsilane. The ordinary cross polarization (CP) pulse sequence was used, where the contact time was 5.0 ms. The recycle time was 15 s, except for the measurement of crystalline pNA-*d* (3000 s).

^{31}P and ^{27}Al MAS NMR measurements were carried out by a Bruker MSL400 spectrometer with a static magnetic field strength of 9.4 T. Larmor frequencies of ^{31}P and ^{27}Al were 161.98 and 104.26 MHz, respectively. A Bruker MAS probehead was used with a 4-mm zirconia rotor. The spinning rates of the sample were set at 4.0 and 8.0 kHz for ^{31}P and ^{27}Al, respectively. Chemical shifts were expressed with respect to 85% H_3PO_4 and 1.0 M $Al(NO_3)_3$ aqueous solution for ^{31}P and ^{27}Al, respectively. The pulse sequences used for ^{31}P NMR spectra were cross polarization (CP) and single pulse (SP) both with high-power ^1H decoupling. The contact time of CP was set at 3.0 ms, and the recycle time for both CP and SP was 20 s. For ^{27}Al, the single pulse sequence (SP) with high-power ^1H decoupling was used. The recycle time was 3.0 s.

^2H NMR spectra were measured by a Bruker MSL400 spectrometer with a static magnetic field strength of 9.4 T. The spectra were recorded at 61.42 MHz, using a Bruker broadband probehead with a solenoid coil for static samples. The quadrupole echo pulse sequence was used, where the latter half of the echo signal was acquired and Fourier transformed. The 90° pulse width was 3.1 μs and the time interval between the two pulses was set at 15 μs. The recycle time was between 1 and 10 s, depending on the sample temperature. The sample temperature was varied from 149 to 433 K. The temperature of the sample was calibrated by using CD_3OD.[23] Spectra were presented with the signal of D_2O being 0 Hz.

^2H line-shape simulations were carried out with the MXET1 program (a descendant version of MXQET),[24] which was kindly provided by R. R. Vold. The program was run on an IBM PC/AT compatible personal computer.

Results and Discussion

^{13}C MAS NMR Spectra. Figure 1 shows ^{13}C CP/MAS NMR spectra of pNA-*d* and $AlPO_4$-5/pNA-*d*. The sample of crystalline pNA-*d* has isotropic peaks at 113.3 (C(2,6)-H), 127.7 and 128.5 (C(3,5)-H), 136.3 (C(4)−NO_2), and 155.4 ppm (C(1)−NH_2), as shown in Figure 1A. The sample of 5.0 mass % has isotropic peaks at 113.7, 127.3, 138.8, and 154.3 ppm (Figure 1B), while the sample of 10.1 mass % has peaks at 113.7, 127.5, 136.5, 138.5, and 154.4 ppm (Figure 1C). Those shift values are listed in Table 1, together with some literature data.

Strong intermolecular hydrogen bonds are formed in crystalline pNA-*d* solid.[25,26] The $AlPO_4$-5/pNA-*d* sample of 5.0 mass % shows low-frequency shifts in C(1)−NH_2 and C(3,5)−H and high-frequency shift in C(4)−NO_2, compared with crystalline pNA-*d*. Similar shifts are observed in ZSM-5/pNA, where hydrogen bonding interaction between pNA molecules is decreased by the inclusion.[18,19] Therefore, the above shifts observed in the sample of 5.0 mass % indicate that inclusion in the nanospace causes weakening of the hydrogen bonds. The intensities of the spinning sidebands reflect the magnitude of the chemical shift anisotropy when comparison is made between the spectra measured at the same spinning rate. They are much lower in the sample of 5.0 mass % than in crystalline pNA-*d*, indicating that pNA-*d* undergoes molecular motions in the nanospace. The magnitude of the chemical shift anisotropy is decreased by the motion.

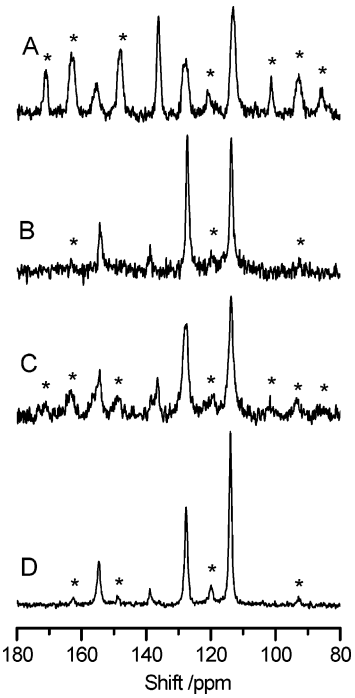

Figure 1. ^{13}C CP/MAS NMR spectra of (A) pNA-*d* at 298 K, (B) $AlPO_4$-5/pNA-*d* of 5.0 mass % at 298 K, and $AlPO_4$-5/pNA-*d* of 10.1 mass % at (C) 298 and (D) 340 K. The spinning rates were 3.5 kHz. The spinning sidebands are marked by an asterisk.

TABLE 1: ^{13}C Chemical Shifts

sample[a]	*T*/K	C(1)−NH_2	C(2,6)−H	C(3,5)−H	C(4)−NO_2
pNA[b]	298	155.4	113.5	127.7, 128.7	136.3
pNA-*d*	298	155.4	113.3	127.7, 128.5	136.3
$AlPO_4$-5/pNA-*d* (5.0 mass%)	298	154.3	113.7	127.3	138.8
$AlPO_4$-5/pNA-*d*	298	154.4	113.7	127.5	136.5, 138.5
(10.1 mass%)	340	154.7	114.0	127.7	138.9
ZSM-5/pNA (6.8 mass%)[b]	298	154.6	113	127	138.4
FSM-16/pNA-*d* (10 mass%)[c]	298	154.9	113.9	126.8	137.8

[a] The loading amount is described in parentheses with respect to the total mass. [b] Reference 18. [c] Reference 22.

The sample of 10.1 mass % has relatively broad peaks, as shown in Figure 1C. The C(4)−NO_2 signal is split into two peaks at 136.5 and 138.5 ppm. The former peak agrees to pNA-*d*, while the latter agrees to the sample of 5.0 mass %. The C(1)−NH_2 signal also appears to consist of two signals: one is similar to pNA-*d*, and the other is similar to the sample of 5.0 mass %. These facts suggest that a portion of molecules form intermolecular hydrogen bonds. In contrast to the sample of 5.0 mass %, many spinning sidebands are observed, although their intensities are smaller than those for crystalline pNA-*d*. The interaction between the guest molecules suppresses the molecular motion considerably.

At 340 K, the sample of 10.1 mass % shows a spectrum similar to the sample of 5.0 mass % at 298 K, as shown in Figure 1D. Each signal becomes sharp. The signal at 136.5 ppm disappears as well as the shoulder around 155 ppm. The intensities of the spinning sidebands become low. These changes suggest that molecular motion becomes fast and that the intermolecular hydrogen bonds are broken.

^2H NMR Spectra. Figure 2 shows ^2H NMR spectra of $AlPO_4$-5/pNA-*d* of 10.1 mass % at several temperatures. The Pake doublet pattern is observed at low temperatures, and this pattern is not changed below 209 K. The doublet has a

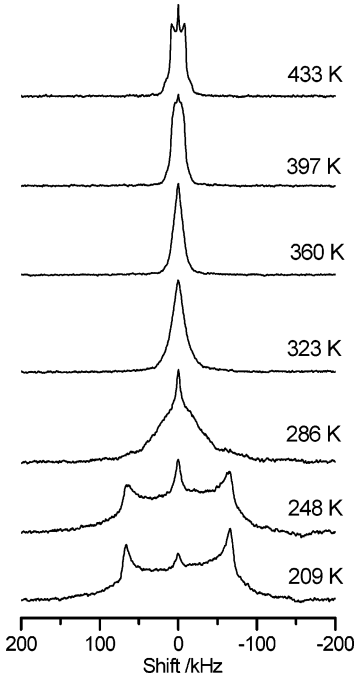

Figure 2. ^{2}H NMR spectra of $AlPO_4$-5/pNA-*d* of 10.1 mass %.

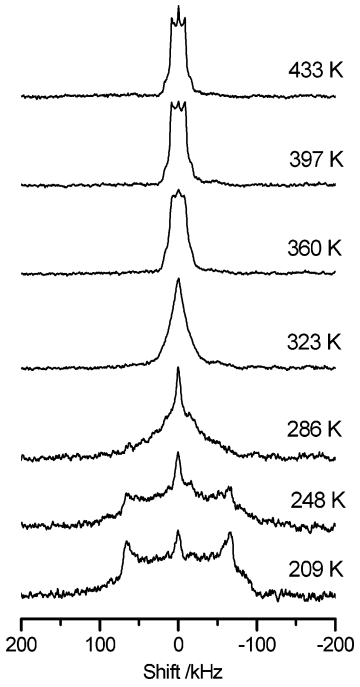

Figure 3. ^{2}H NMR spectra of $AlPO_4$−5/pNA-*d* of 5.0 mass %.

quadrupole coupling constant (QCC) of 180 kHz and an asymmetric factor (η_Q) of 0. The resolved doublet can be ascribed to pNA-*d* molecules in a rigid state. The relatively sharp signal at the shift of 0 kHz is ascribed to pNA-*d* on the outer surface, whose intensity is less than 2%. This component is excluded in the discussion below. With an increase in temperature, the central region grows up and the doublet disappears. No fine structures are observed in the temperature range from 286 to 360 K. Above 360 K the central signal is broadened gradually, and at 415 K a narrower Pake doublet pattern is recognized. The spectrum at 434 K shows a pattern with the effective QCC of 24 kHz and the effective η_Q of 0.

Figure 3 shows ^{2}H NMR spectra of $AlPO_4$-5/pNA-*d* of 5.0 mass %. They show a similar temperature dependence to the

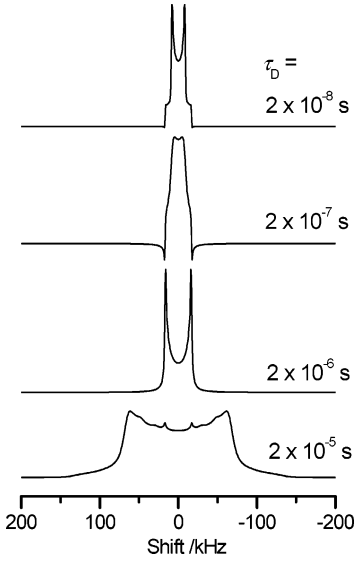

Figure 4. Calculated ^{2}H NMR spectra for the six-site jump model.

sample of 10.1 mass %. However, a similar spectrum is observed in the sample of 5.0 mass % at the lower temperature than in the sample of 10.1 mass %. This means that the motion of pNA-*d* molecules is faster in the sample of 5.0 mass % than in the sample of 10.1 mass %. These results agree with the ^{13}C NMR results.

Analysis of ^{2}H NMR Spectra. The observed ^{2}H NMR spectra are analyzed theoretically to derive the mode and the rate of the motion of pNA-*d* in the nanospace. $AlPO_4$-5 has one-demensional channels of 12-membered rings with a diameter of 0.73 nm.[9] On the other hand, the length of the pNA molecule is about 1 nm. Thus, the channel dimension prohibits the perpendicular orientation of the C_2 axis of the molecule to the channel axis.

The simplest orientation is that the molecular axis is parallel to the channel axis. The molecule can reorient around the molecular C_2 axis. According to the C_6 symmetry of the channel cross section, the most plausible motion is a six-site jump. Thus, we have attempted to simulate the spectra by assuming the six-site jump, and some calculated spectra are shown in Figure 4. A narrower Pake doublet pattern is obtained at the fast motional limit. When η_Q is 0 in a rigid state, the effective QCC is reduced by a factor of $(3\cos^2\theta - 1)/2$ and the effective η_Q is 0 at the fast limit. The θ value is defined as the angle between the C−D vector and the axis of the jump. In the present case, $\theta = 60°$, and thus the effective QCC should be 23 kHz, which agrees excellently with the observed value (24 kHz). However, the calculated spectra show characteristic fine structures in the intermediate temperature range. Because the observed spectra show no fine structures in this temperature range, the six-site jump model is not suitable.

The similar reason excludes the possibilities of a three-site jump, a twelve-site jump, and so on. The symmetry of the channel cross section also makes these motions unfavorable. A two-site jump, or 180° flip-flop, is also excluded because this motion results in much different line shapes.[19]

The absence of the fine structure in the intermediate temperature range was observed in benzene-d_6, cyclohexane-d_{12}, *n*-hexane-d_{14} in KL zeolite,[17] and acetonitrile-d_3 in $AlPO_4$-5.[18] In these systems, exchange between an adsorbed state and an isotropically rotating state takes place. However, pNA-*d* molecules cannot rotate isotropically in the channel of $AlPO_4$-5 because of the limited space. Therefore, the exchange model is excluded.

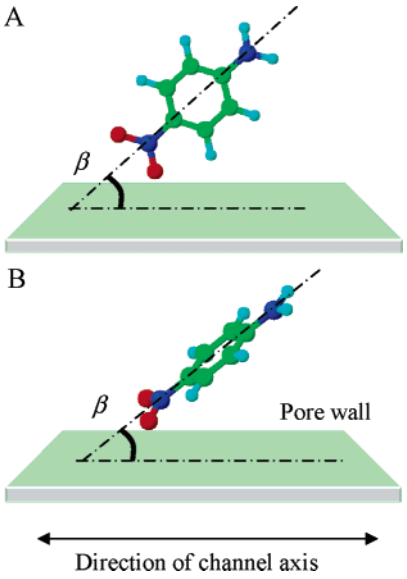

Figure 5. Models of the orientation of pNA with respect to the pore wall in the micropore. (A) The molecular plane is perpendicular to the pore wall and (B) the molecular plane is inclined to the channel axis. The pore wall is approximated as a flat plane.

The pNA-*d* molecule might interact with the framework. The functional group like NO_2 or NH_2 might locate near the inner surface. It is well-known that H_2O coordinates to Al rather strongly, forming 5-fold- and 6-fold-coordinated Al atoms.[27] Thus, 4-fold-coordinated Al atoms (Al(IV)) in the framework play the role of a Lewis acid. Therefore, the NO_2 group might coordinate to Al. In this case, the molecular axis is inclined to the channel axis.

First, the molecular plane is assumed to be perpendicular to the channel wall, as is schematically shown in Figure 5A. When the molecular axis is inclined to the channel axis by an angle β, the C−D vector has an angle of $60° \pm \beta$ to the channel axis. In other words, the C−D vector has two orientations on each site. The 180° flip around the molecular C_2 axis can exchange the two orientations. Because the channel cross section has C_6 symmetry, the molecule undergoes a six-site jump around the channel axis. Consequently, there exist 12 orientations in the C−D vector. The NO_2 group of the pNA molecule might coordinate to Al. When the molecule jumps, the coordination to Al is broken and the molecule can take any other orientations with an equal probability. Thus, all the exchange rates are assumed to be the same among the 12 orientations. Figure 6 shows simulated spectra, which can well explain the observed spectra in Figure 2.

Next, the molecular plane is assumed to be inclined to the channel axis, as is schematically shown in Figure 5B. The inclined molecule undergoes a six-site jump, and totally 12 orientations are present for the C−D vector. We have attempted to calculate the spectra at several β values, in which β is the angle between the molecular axis and the channel axis. Figure 7 shows calculated spectra for $\beta = 15°$. The spectra in the intermediate temperature range cannot be reproduced, although the spectra at high temperatures can be reproduced.

In conclusion, the molecular orientation shown in Figure 5A satisfactorily explains the observed ^{2}H NMR spectra. The same motional mode can be applied to the sample of 5.0 mass % because similar ^{2}H NMR spectra are observed. The mean residence time, τ_D, is plotted as a function of inverse temperature in Figure 8. The molecular motion is faster in the sample of 5.0 mass % than in the sample of 10.1 mass %. The interaction

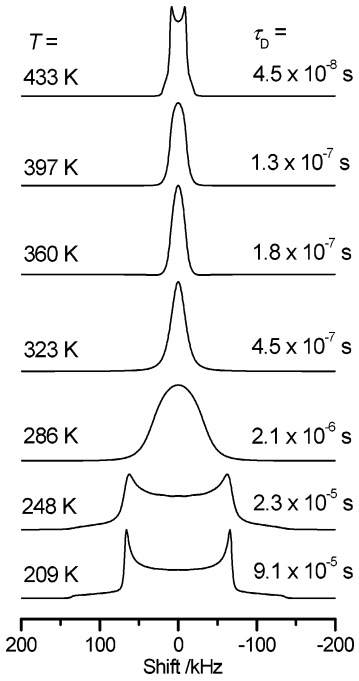

Figure 6. Simulated ^{2}H NMR spectra for $AlPO_4$-5/pNA-*d* of 10.1 mass %, assuming the molecular orientation shown in Figure 5A.

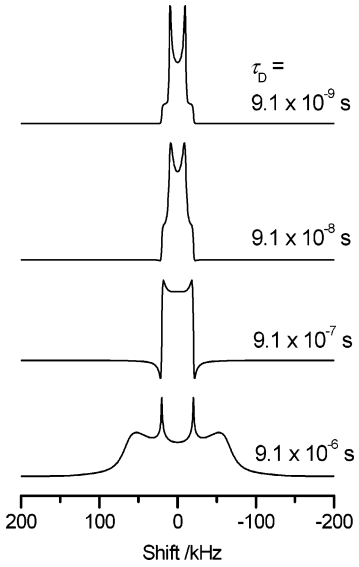

Figure 7. Calculated ^{2}H NMR spectra for the molecular orientation shown in Figure 5B.

between the guest molecules suppresses the molecular motion slightly. The mean residence time can be assumed to obey the Arrhenius law described below:

$$\tau_D = \tau_0 \exp(E_a/RT) \quad (1)$$

where τ_0 is a mean residence time at the infinite temperature, E_a is an apparent activation energy, R is the gas constant, and T is temperature. From the plot in Figure 8, $\tau_0 = 2.8 \times 10^{-11}$ s and $E_a = 26.9 \pm 1.0$ kJ mol^{-1} for the sample of 10.1 mass % and $\tau_0 = 2.1 \times 10^{-11}$ s and $E_a = 26.2 \pm 0.9$ kJ mol^{-1} for the sample of 5.0 mass %.

^{31}P and ^{27}Al MAS NMR Spectra. The chemical environments of P atoms in the framework have been studied by ^{31}P MAS NMR. The spectrum of dehydrated $AlPO_4$-5 shows two signals at −28.1 and −31.8 ppm, whose intensity ratio is about 1:1, as shown in Figure 9A. The SP spectrum of $AlPO_4$-5/pNA-*d*

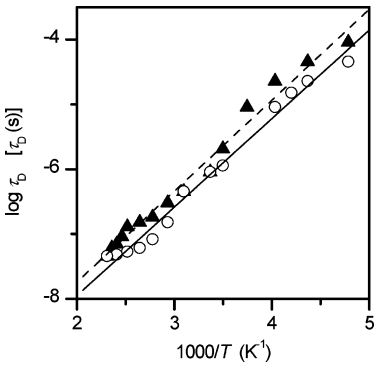

Figure 8. The mean residence times of pNA-*d* molecules in the $AlPO_4$-5/pNA-*d* samples of (○) 5.0 and (▲) 10.1 mass %.

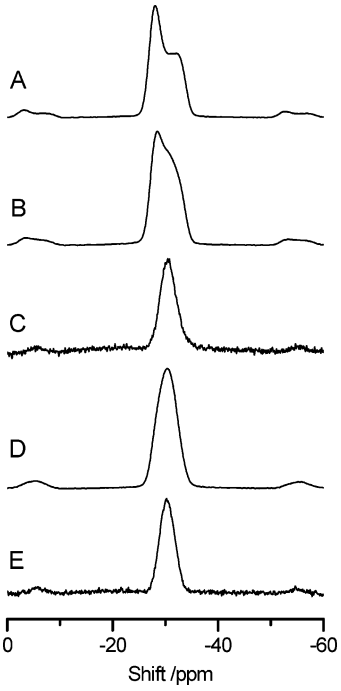

Figure 9. ^{31}P MAS NMR spectra of (A) dehydrated $AlPO_4$-5 measured by SP, (B) $AlPO_4$-5/pNA-*d* of 5.0 mass % measured by (B) SP and (C) CP, and $AlPO_4$-5/pNA-*d* of 10.1 mass % measured by (D) SP and (E) CP.

of 5.0 mass % consists of more than one component (Figure 9B). On the other hand, the CP spectrum has only one component at −30.4 ppm. Only ^{31}P spins in the neighborhood of the guest molecules are detected in the CP spectrum, because polarization of ^{1}H spins in the guest molecules is transferred to ^{31}P spins in the framework during the CP process. The dehydrated host containing no pNA-*d* gives no signal in the CP spectrum, because it contains no ^{1}H spins. On the other hand, all ^{31}P spins are detected in the SP spectrum. The difference between the SP and CP spectra originates from the host containing no pNA-*d*. Consequently, the SP spectrum in Figure 9B consists of three components: one from the region containing pNA-*d* and the other two from the host containing no pNA-*d*. We deconvolute the spectrum, assuming Gaussian line shapes, as shown in Figure 10A, and the parameters are listed in Table 2. The signal at −30.4 ppm is ascribed to the region containing pNA-*d*, whereas the signals at −28.1 and −31.9 ppm come from the host containing no pNA-*d*. These results demonstrate that the guest molecules are not distributed in the host homogeneously. The results indicate that 27% of the host contains pNA-*d*, while the other region is unoccupied.

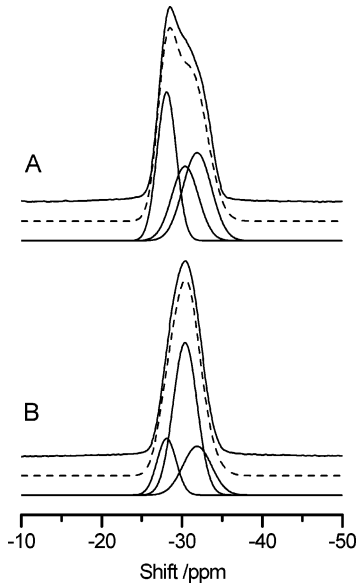

Figure 10. Deconvoluted results of ^{31}P SP/MAS NMR spectra of the $AlPO_4$-5/pNA-*d* samples of (A) 5.0 and (B) 10.1 mass %. The observed, calculated, and component spectra are drawn from top to bottom.

TABLE 2: Parameters Obtained from the ^{31}P MAS NMR Spectra

sample	mode	shift/ppm	fwhm/Hz	intensity/%
$AlPO_4$-5	SP	−28.0	450	52
		−31.8	680	48
$AlPO_4$-5/pNA-*d*	SP	−28.1[a]	450	39
(5.0 mass %)		−30.4	630	27
		−31.9[a]	680	34
	CP	−30.4	630	100
$AlPO_4$-5/pNA-*d*	SP	−28.1[a]	450	17
(10.1 mass %)		−30.3	570	59
		−31.9[a]	680	24
	CP	−30.3	570	100

[a] From the host containing no pNA-*d*.

Spectra D and E in Figure 9 show the SP and CP spectra, respectively, of $AlPO_4$-5/pNA-*d* of 10.1 mass %. The full width at half-maximum (fwhm) of the signal in the SP spectrum is 750 Hz, which is broader than that of the CP spectrum (570 Hz). The SP spectrum consists of three components, similar to the sample of 5.0 mass %. We deconvolute the spectrum, as shown in Figure 10B, and the obtained parameters are listed in Table 2. The results indicate that 59% of the host contains pNA-*d*, while the other region is unoccupied. The occupied region in $AlPO_4$-5/pNA-*d* of 10.1 mass % is about twice that in the sample of 5.0 mass %. This indicates again the inhomogeneous distribution of pNA-*d*.

Figure 11 shows ^{27}Al MAS NMR spectra. In the ambient conditions, $AlPO_4$-5 is hydrated, and its ^{27}Al spectrum has three signals ascribed to 4-fold- (Al(IV)), 5-fold- (Al(V)), and 6-fold-coordinated Al (Al(VI)) at 39, 6, and −13 ppm, respectively, as shown in Figure 11A. Al(V) and Al(VI) are formed by coordination of water molecules. The dehydrated material has only one signal at 36.1 ppm (Figure 11B), which represents Al(IV) ($Al(OP)_4$). The $AlPO_4$-5/pNA-*d* samples of 5.0 and 10.1 mass % have a signal at 35.8 and 35.3 ppm, respectively, both of which are ascribed to Al(IV). Consequently, the pNA-*d* molecule does not coordinate to Al like H_2O. The slight shift of the signal indicates that distortion of the framework is caused by accommodation of pNA-*d*.

Orientation and Dynamics of Guest Molecules. $AlPO_4$-5 has one-demensional channels of 12-membered rings with a

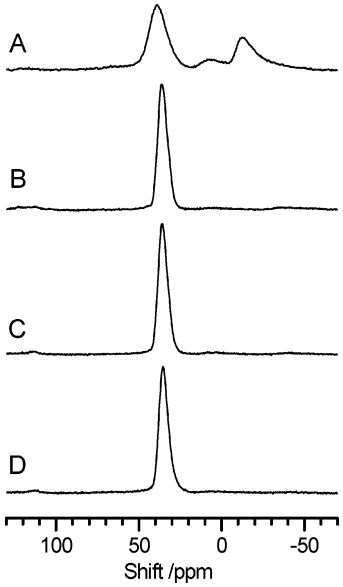

Figure 11. ^{27}Al SP/MAS NMR spectra of (A) hydrated $AlPO_4$-5, (B) dehydrated $AlPO_4$-5, (C) $AlPO_4$-5/pNA-*d* of 5.0 mass %, and (D) $AlPO_4$-5/pNA-*d* of 10.1 mass %.

diameter of 0.73 nm.[9] One unit of $AlPO_4$-5 has the length of 0.85 nm, and the length of the pNA molecule is about 1 nm. The amounts of pNA-*d* are 5.0 and 10.1 mass %, which correspond to 0.31 and 0.65 molecules per unit cell, respectively. The maximum loading amount is roughly 13 mass %. The maximum SHG intensity was obtained at about 13 mass % in $AlPO_4$-5/pNA.[1]

The incorporation of pNA-*d* in the channel of $AlPO_4$-5 causes slight distortion of the framework, as demonstrated by the ^{31}P and ^{27}Al MAS NMR spectra. The ^{31}P spectra demonstrate inhomogeneous distribution of pNA-*d* molecules in the channel. Two types of domains are formed: one contains pNA-*d* molecules while the other does not. Approximately 27% and 59% of the host are used to incorporate pNA-*d* molecules in the samples of 5.0 and 10.1 mass %, respectively. The ^{27}Al NMR spectra suggest that pNA-*d* molecules do not coordinate to Al strongly like H_2O.

Intermolecular hydrogen bonds are formed in crystalline pNA. The ^{13}C NMR results indicate that inclusion in the nanospace causes weakening of the hydrogen bonds. However, the intermolecular hydrogen bonds are formed between a portion of the guest molecules when the loading level is high. With an increase in temperature the hydrogen bond is broken due to the molecular motion. The molecular motion in the nanospace is indicated by the small intensities of the spinning sidebands. This motion is a little bit suppressed at the high loading level due to the interaction between the guest molecules.

The molecular orientation shown in Figure 5A satisfactorily explains the observed ^2H NMR spectra. The molecular axis of pNA-*d* is inclined to the channel axis by 37°. The molecular plane is perpendicular to the inner wall. One of the O atoms in the NO_2 group might coordinate to Al. Al can work as a type of Lewis acid site, because H_2O coordinates to Al rather strongly. Because the interaction of the guest molecule with Al is weak and the guest molecule is jumping between the sites, we cannot detect Al coordinated by the guest molecule by ^{27}Al NMR. The channel cross section has C_6 symmetry, and the C−D vector in a pNA-*d* molecule has two orientations for each site. Thus, the guest molecule jumps among 12 sites or 12 orientations. The low-loading sample shows faster motion than the high-loading sample, suggesting that the guest−guest interaction hinders the motion.

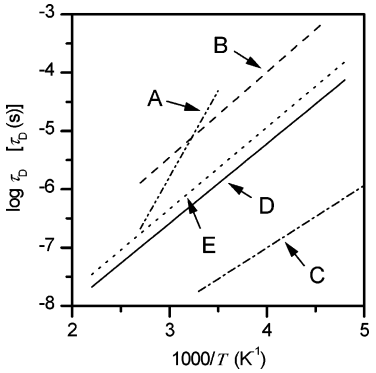

Figure 12. Comparison of the mean residence times of the guest molecules in microporous materials; (A) ZSM-5/pNA-*d*, (B) KL/benzene-d_6, (C) $AlPO_4$-5/acetonitrile-d_3, in addition to $AlPO_4$-5/pNA-*d* of (D) 5.0 and (E) 10.1 mass %.

Figure 12 shows the mean residence times for several systems. The motion of acetonitrile-d_3[21] is faster than that of pNA-*d* in $AlPO_4$-5. The molecular size of acetonitrile-d_3 is smaller than that of pNA-*d*, and the basicity of the former is smaller than that of the latter. The pNA-*d* molecules undergo 180° flip-flop motion in the channel of ZSM-5.[19] This motion is slower than that in the channel of $AlPO_4$-5. The smaller channel dimension of ZSM-5 makes the motion of the guest molecules slow. The motion of benzene-d_6 in KL zeolite[17] is slower than that of pNA-*d* in $AlPO_4$-5. Benzene molecules interact with K^+ ions strongly, which suppresses the motion of benzene molecules. In conclusion, the motion of the guest molecules is affected by the size of the nanospace as well as the property of the adsorbed site.

Conclusion

We have studied the motion of pNA-*d* molecules in the micropores of $AlPO_4$-5 by means of solid-state NMR. We have measured ^{13}C MAS and ^2H NMR spectra of the guest molecules and ^{31}P and ^{27}Al MAS NMR spectra of the host framework, and have obtained the following conclusions:

(1) The ^{31}P MAS NMR spectra demonstrate that pNA-*d* molecules distribute rather inhomogeneously in the channel. The ^{27}Al MAS NMR spectra suggest that pNA-*d* molecules do not coordinate to Al strongly like H_2O.

(2) The ^{13}C MAS NMR spectra indicate that the intermolecular hydrogen bonds are formed between a portion of the guest molecules only when the loading level is high. They are not formed at the low loading levels.

(3) The ^2H NMR spectra are successfully analyzed, elucidating the orientation and the motion of the guest molecules. The molecular axis of pNA-*d* is inclined to the channel axis, and the molecular plane is perpendicular to the inner wall. One of O atoms in the NO_2 group might coordinate to Al, although the coordination is very weak. The channel cross section has C_6 symmetry, and the C−D vector in a pNA-*d* molecule has two orientations for each site. Thus, the guest molecule jumps among 12 sites or 12 orientations.

(4) The ^{13}C MAS NMR spectra and ^2H NMR spectra demonstrate that the low-loading sample shows faster motion than the high-loading sample, suggesting that the guest−guest interaction hinders the motion.

(5) The mean residence times of the molecules are estimated from the ^2H NMR spectra. The obtained parameters are $\tau_0 = 2.8 \times 10^{-11}$ s and $E_a = 26.9 \pm 1.0$ kJ mol^{-1} for the sample of

10.1 mass % and $\tau_0 = 2.1 \times 10^{-11}$ s and $E_a = 26.2 \pm 0.9$ kJ mol^{-1} for the sample of 5.0 mass %. The motion of the guest molecules is affected by the size of the nanospace as well as the property of the adsorbed site.

Acknowledgment. We thank Dr. K. Suzuki of AIST for the supply of $AlPO_4$-5. We acknowledge the late Prof. R. R. Vold for kindly providing us source programs of MXET1. We also thank Dr. M. Sugie of AIST for installing the program in an IBM PC/AT compatible personal computer.

References and Notes

(1) Cox, S. D.; Gier, T. E.; Stucky, G. D.; Bierlein, J. *J. Am. Chem. Soc.* **1988**, *110*, 2986.

(2) Cox, S. D.; Gier, T. E.; Stucky, G. D.; Bierlein, J. *Solid State Ionics* **1989**, *32/33*, 514.

(3) Cox, S. D.; Gier, T. E.; Stucky, G. D. *Chem. Mater.* **1990**, *2*, 609.

(4) Werner, L.; Caro, J.; Finger, G.; Kornatowski, J. *Zeolites* **1992**, *12*, 658.

(5) Caro, J.; Finger, G.; Kornatowski, J.; Richter-Mendau, J.; Werner, L.; Zibrowis, B. *Adv. Mater.* **1992**, *4*, 273.

(6) Caro, J.; Marlow, F.; Wübbenhorst, M. *Adv. Mater.* **1994**, *6*, 413.

(7) Binder, G.; Scandella, L.; Kritzenberger, J.; Gobrecht, J.; Koegler, J. H.; Prins, R. *J. Phys. Chem. B* **1997**, *101*, 483.

(8) Kinski, I.; Gies, H.; Marlow, F. *Zeolites* **1997**, *19*, 375.

(9) Baerlocher, Ch.; Meier, W. M.; Olson, D. H. *Atlas of Zeolite Framework Types*, 5th ed.; Elsevier: Amsterdam, The Netherlands, 2001; p 34.

(10) Hayashi, S.; Suzuki, K.; Shin, S.; Hayamizu, K.; Yamamoto, O. *Chem. Phys. Lett.* **1985**, *113*, 368.

(11) Hayashi, S.; Suzuki, K.; Hayamizu, K. *J. Chem. Soc., Faraday Trans. 1* **1989**, *85*, 2973.

(12) Satozawa, M.; Kunimori, K.; Hayashi, S. *Bull. Chem. Soc. Jpn.* **1997**, *70*, 97.

(13) Xie, X.; Hayashi, S. *J. Phys. Chem. B* **1999**, *103*, 5956.

(14) Hayashi, S. *J. Phys. Chem.* **1995**, *99*, 7120.

(15) Hayashi, S. *Clays Clay Miner.* **1997**, *45*, 724.

(16) Xie, X.; Hayashi, S. *J. Phys. Chem. B* **1999**, *103*, 5949.

(17) Sato, T.; Kunimori, K.; Hayashi, S. *Phys. Chem. Chem. Phys.* **1999**, *1*, 3839.

(18) Hayashi, S.; Komori, Y. *Stud. Surf. Sci. Catal.* **2001**, *135*, 13P06.

(19) Komori, Y.; Hayashi, S. *Phys. Chem. Chem. Phys.* **2003**, *5*, 3777.

(20) Komori, Y.; Hayashi, S. *Bull. Chem. Soc. Jpn.* **2004**, *77*, 673.

(21) Hayashi, S. *Microporous Mesoporous Mater.* **2003**, *66*, 253.

(22) Komori, Y.; Hayashi, S. *Microporous Mesoporous Mater.* **2004**, *68*, 111.

(23) van Geet, A. L. *Anal. Chem.* **1970**, *42*, 679.

(24) Greenfield, M. S.; Ronemus, A. D.; Vold, R. L.; Vold, R. R.; Ellis, P. D.; Raidy, T. E. *J. Magn. Reson.* **1987**, *72*, 89.

(25) Trueblood, K. N.; Goldish, E.; Donohue, *J. Acta Crystallogr.* **1961**, *14*, 1009.

(26) Colapietro, M.; Domenicano, A.; Mariciante, C.; Portalone, G. *Z. Naturforsch.* **1982**, *37b*, 1309.

(27) Fyfe, C. A.; Wong-Moon, K. C.; Huang, Y. *Zeolites* **1996**, *16*, 50.